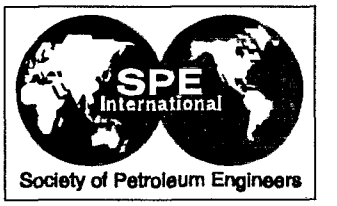


Δ

SPE 48926

# Effects of Shear Planes and Interfacial Slippage on Fracture Growth and Treating Pressures

R. D. Barree, SPE, and P. H. Winterfeld, SPE, Marathon Oil Company



This paper was prepared for presentation at the 1998 SPE Annual Technical Conference and Exhibition held in New Orleans, Louisiana, 27–30 September 1998.



## Abstract

The equations used in current hydraulic fracture simulators are based on plane-strain solutions, or use a complete surface integral solution for fracture width. Assumptions inherent in these solutions control the stress field surrounding the fracture tip and the stress intensity developed at the tip which, in turn, controls the rate of fracture growth and containment and the predicted net pressure. The overriding assumption made in these solutions is that the entire rock mass is elastically coupled so that all stresses and deformations interact.

Many reservoirs that are hydraulically fractured are susceptible to complex fracturing which can invalidate the assumption of elastic coupling. Microseismic monitoring of fracture growth indicates that energy is lost to shear failures around the fracture. During hydraulic fracturing high fluid pressures, often exceeding both the minimum and maximum horizontal stress (fissure opening pressure), result in the reduction of the normal stress acting across natural fissures. This allows free shear or slippage along natural fracture planes in reservoirs or cleats in coal. When shear or slippage occurs elastic coupling in the rock mass is lost and each shear block deforms as a separate unit. This shear decoupling results in tremendous reduction in created fracture width and leads to high frictional pressures (low transmissibility) and difficulty in placing proppant, especially large proppant.

The purpose of this work is to suggest that current fracture models are missing what could be a dominant containment mechanism in the fracturing of fissured reservoirs, coals, and soft rocks and that further work is required to fully understand the implications of slippage and shear failure on treatment designs.

## Introduction

Fracture geometry models currently in use are based on closed-form analytical solutions and surface integral solutions of linear-elastic displacement equations. The equations applied are founded on similar assumptions.[1-5] The equations are commonly solved for specific geometries like the plane-strain linear crack, or circular "penny" crack. Solutions for specific geometries are embedded in fracture geometry models, which are forced to make simplifying assumptions to conform to the closed-form solutions.[6-8] The width solutions generated by these models fail, or diverge from observed widths, when the actual fracture geometries deviate from the assumed geometries.[9] More advanced pseudo three-dimensional models attempt to minimize this effect by coupling width solutions in orthogonal planes.[10] Planar three-dimensional models go one step further in reducing the reliance on an assumed fracture geometry by solving the surface integral form of the width equation without external geometry constraints.[9, 11]

All these solutions, however, assume that the entire rock mass acted on by the frac-fluid pressure is elastically coupled, along with the assumption of linear-elastic deformation. Under the assumption of elastic coupling, a load applied at any point on the surface of a semi-infinite linear-elastic medium will generate a displacement normal to the surface at all points on the surface. The magnitude of the displacement diminishes with the inverse of the distance from the applied load. The width distribution which results from the application of a pressure, or a system of applied loads distributed over some area of the surface, results from the integration of all displacements caused by all loads over the entire surface.[5]

## Plane Strain and Surface Integral Width Solutions

The plane-strain solution is a special case where a load distributed over a characteristic fracture 'height' extends to infinite 'length'. This results in a displacement that varies along the fracture height but is constant along the fracture length. Therefore, all displacements (strains) occur in a plane normal to the fracture surface. Real fractures, however, are not infinite in length. This leads to the width errors observed in simple models, which are commonly associated with low aspect ratios (length similar to height). If width errors were only associated with application of the plane-strain model,

more advanced geometry models should adequately describe the observed width distribution. However, field observation and modern fracture diagnostic tools suggest that width profiles and observed height containment differ strikingly from predictions.[12, 13]

## Effects of Shear Planes

Microseismic monitoring of fracture growth points to a mechanism that impacts both the width distribution and the stress concentration developed at the fracture perimeter, hence the degree of containment. Microseisms occur as a result of shear slippage in the disturbed rock mass.[14] Shear movement is resisted by friction within the rock which is a direct result of the magnitude of normal forces acting on the shear plane. If the normal forces are reduced by pressurized fluid invasion along the shear plane, slippage can occur. Once the rock mass slips, strain energy cannot be elastically transmitted to the rock adjacent to the slippage plane. This mechanism alone, which is indicated by direct observation, invalidates all plane-strain assumptions and the application of a complete surface integral solution.

**Width Solution with Shear Dampening.** As an illustration of the influence of the applied load distribution on process zone stresses and width profiles, a series of static displacement and stress solutions were carried out using a surface-integral model. The model calculates displacements, or fracture widths, in areas where load is specified. Outside the fracture, where displacement is known, stresses are calculated. In practice, the assumed open area of the fracture is assigned some "net" pressure distribution and the unbroken rock mass surrounding the fracture is assigned a zero-displacement condition. Figure 1 is a plot of the calculated width profile along the "height" of an approximately plane-strain fracture with a constant net pressure of 1000 psi. Resultant tensile stresses in the bounding zone around the fracture (process zone) are also shown.

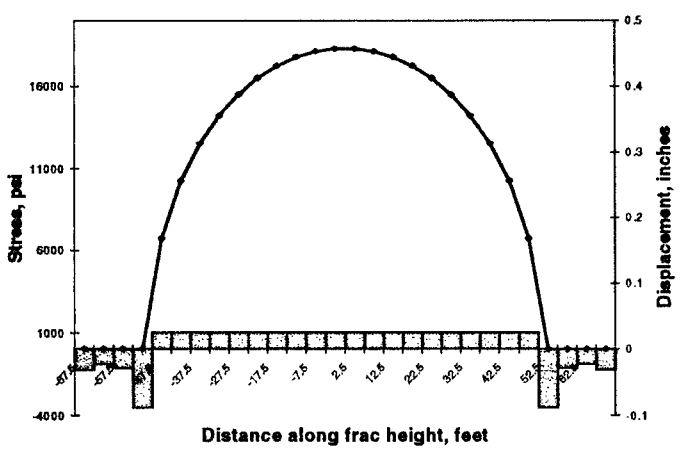


**Figure 1: Width and stress profiles for plane-strain linear crack**

Note that the commonly expected elliptical width profile results, with a maximum width at the fracture center of approximately 0.45 inches. This agrees with the plane-strain linear crack solution of Sneddon.[3] The maximum tensile stress in the boundary (process) zone at the fracture tips exceeds 3500 psi. The tensile stress in the surrounding rock falls off quickly outside the fracture perimeter. The increase in tensile stress at the outer boundary of the model grid reflects a stress concentration resulting from truncation of the grid. If the numerical grid were extended further, the stresses are found to decrease monotonically to zero with increasing distance.

**Examples of Shear Dampening.** To illustrate the impact of the plane-strain assumption, the fracture was segmented into 20 foot long sections. The same 1000 psi net pressure was applied to one 20 foot section. Figure 2 is a plot of the resulting width and stress profile for a 20 foot long section of fracture with free slip along shear planes at each end. Two things are immediately apparent: The fracture width created by the same applied load is 46% of the plane-strain case, and the tensile stress concentration at the fracture boundary is reduced by 45%. For the same rock properties and strengths, fracture containment will be significantly better for the latter case (lower process zone stress or stress intensity).

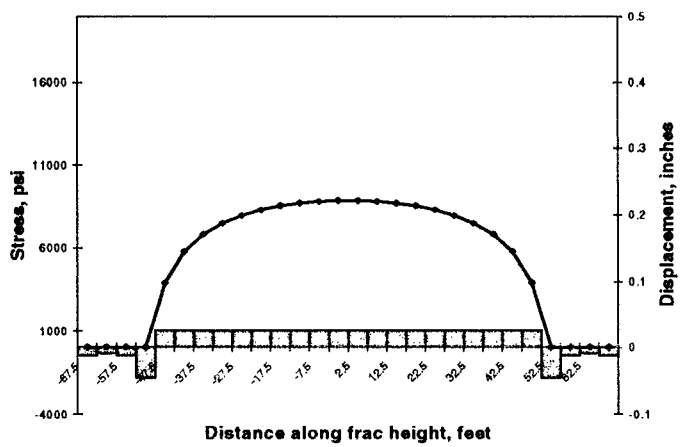


**Figure 2: Width and stress profiles for 20' linear crack segment**

## Shear dampening radius

In real rock masses there is no reason to assume that natural fractures or incipient shear planes will always transept the fracture height or segment the fracture along its length. Shear fractures may occur in cross-cutting sets, more-or-less uniformly distributed over the fracture surface. In this instance, elastic coupling is lost in all directions (height and length) rather than just along the length of the fracture. To simulate this instance we define a "shear dampening radius" ($S_d$), which is the maximum radial distance from a point of applied load that elastic coupling can be maintained. In the surface integral solution, the displacement at each point is found by integrating the load applied within this radius, and ignoring any loads outside the dampening radius.

The influence of shear dampening on boundary stresses and width profiles is shown in Figure 3. The plot shows width and stress distributions for a uniform pressure over the entire

fracture area with a shear dampening radius of 20 feet ($S_d$=20). Comparing these results with the 20 foot linear segment (Figure 2) and the plane-strain solution (Figure 1) for the same applied load shows a significant effect on maximum created width, width profile with height, and process zone stress. With more shear fracturing, or smaller values of $S_d$, the system tends to generate narrower fracture widths and better height containment. Both these conditions are commonly inferred from field observations.

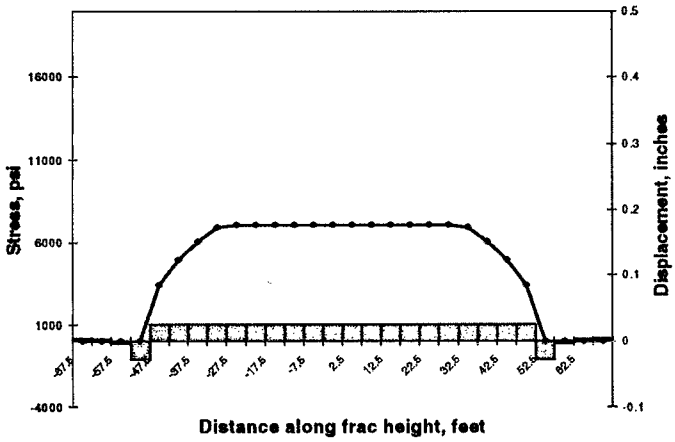


**Figure 3: Width and stress profiles for 20' shear-dampening radius**

Figure 4 is a plot of width and stress for values of $S_d$ ranging from infinity (the plane-strain case) to 10 feet. Some interesting effects are apparent. For large values of $S_d$ the influence of the tensile stresses along the fracture boundary are felt within the body of the fracture. The tensile stresses resist fracture opening and result in a decreased width. When $S_d$ becomes small enough that boundary zone stresses are not transmitted to the center of the fracture, an odd width profile results, where the center of the fracture is very wide. Clearly the approximation made here is not exact. A solution allowing partial slippage at each shear plane and gradual dampening of the displacement field with distance is preferable to a sharp cutoff, but the simplified method used illustrates the effect.

Note that as $S_d$ decreases the calculated fracture width drops from 0.45 inches to 0.10 inches and the width profile changes from an elliptical shape to a nearly flat profile. Maximum tensile stress in the fracture process zone decreases from 3500 psi to 500 psi. This elimination of stress at the fracture boundary suggests that improvement in containment can be expected with increasing shear-fracture frequency. It also helps to explain the tendency for net treating pressure to increase with decreasing shear-dampening radius, as more net pressure is required to raise process-zone stresses to the failure point. Smaller fracture widths also lead to an increased importance of viscous gradients in the fracture. This is a significant departure from "tip dominated" models which show little viscous effect.

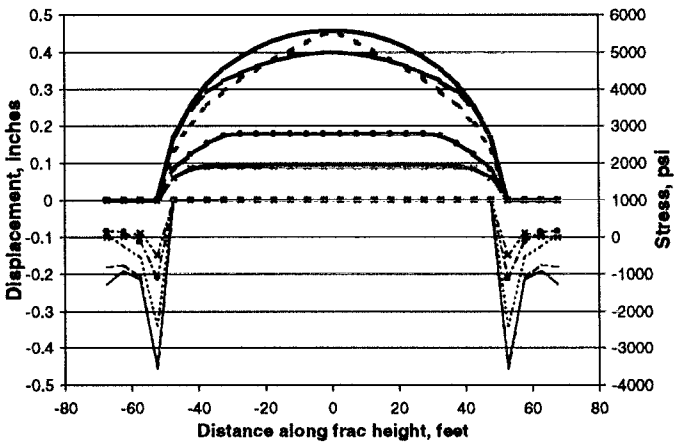


**Figure 4: Summary of widths and stresses for various dampening radii**

## Slippage at Bed Boundaries

A similar condition can occur at bed boundaries. Tiltmeter mapping and seismic monitoring both commonly show instances of horizontal fracture growth, even at great depth, which appear to be related to bed separation.[13,14] A mechanism similar to shear-dampening can be invoked to explain the phenomenon. Possibly as a result of shear-dampening and imperfect elastic coupling, excess stress cannot be transmitted across a bed boundary. The narrow width and improved containment increase the frac fluid pressure. As the increased fluid pressure invades the bed boundary plane the normal stress is reduced. As shown by a typical Mohr-Coulomb failure envelope (Figure 5), as normal stress is reduced the amount of shear stress that can be supported without shear failure (slippage) also decreases. The high fluid pressure acting on the fracture wall increases shear stress along the bed boundary plane while the fluid pressurizing the pore space and bed-boundary plane decreases normal stress, causing slippage to occur. In the case of perfect slip, no stress is transmitted across the interface. In reality, some stress can be transmitted through friction until the interface actually opens and frictional coupling is lost. Fracture growth can only continue across the boundary if the fluid pressure exceeds the stress in the boundary zone and can invade existing cracks or pores in the bounding bed. This phenomenon can lead to frequently observed fracture offsets and bifurcations at bed boundaries.

Bed slip can have large scale effects on fracture geometry. If slippage occurs along a bed boundary, any displacements below the boundary cannot be transmitted across the boundary. The sliding bed boundary then acts as a "wall" separating the fracture into decoupled zones of displacement with each bed segment being displaced only by the pressure acting on it. This effect can be called "shear shadowing" because the rock mass on the opposite side of the "wall" is in a displacement shadow, separated from the remaining rock mass.

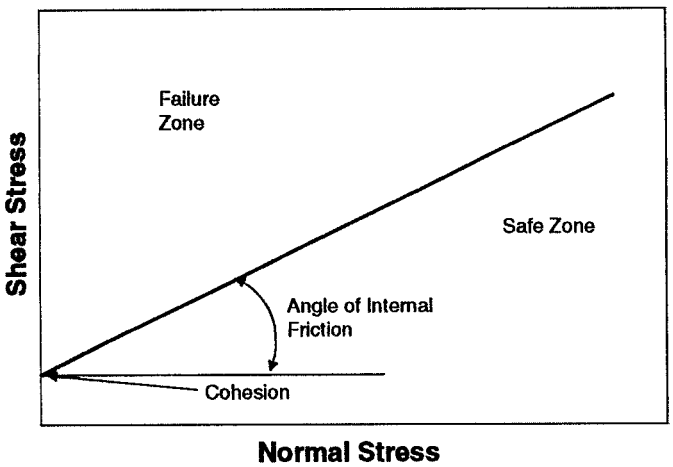


**Figure 5: Typical Mohr-Coulomb failure envelope**

**Effects of Shear Shadowing.** Shear shadowing can be an important consideration in soft rock fracturing, such as frac-packing. The Mohr-Coulomb failure envelope for a typical Gulf Coast unconsolidated sediment can be characterized by an internal angle if friction of 30° and a cohesion value of approximately 300 psi. Depending on depth (normal confining stress) the soft sediment itself can only support a shear stress which is limited by this failure envelope. Higher shear loadings will generate shear failure (slippage) planes within the sand, with the associated reduction in stress concentration in the confining beds.

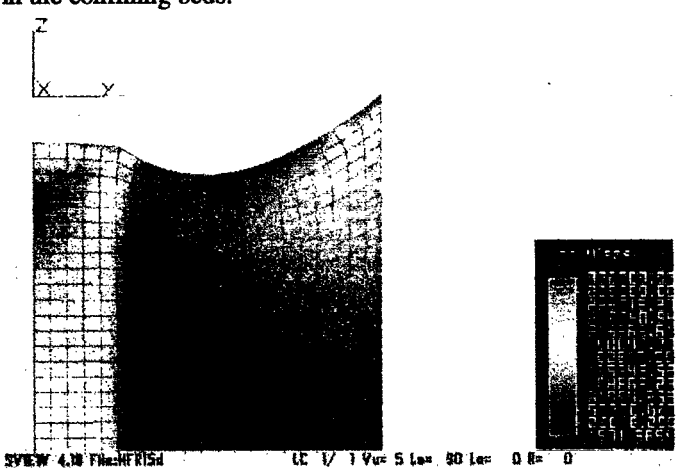


**Figure 6: Displacement and strain energy from FEM solution**

A finite element model (FEM) was run using the commercially available ALGOR software package to analyze displacements (strains) and stresses in a layered system consisting of soft sand (Young's modulus of 0.5e6 psi) and relatively hard silt (Modulus of 5e6 psi) acted upon by a constant net pressure. The system shown in Figure 6 is a soft sand body with a stripe of hard silt in the center. Half of the total sand body is shown in the figure. All displacement and stress profiles are symmetric about the left-hand edge of the figure. A boundary condition specifying no vertical or lateral strain was applied at the outer edge of the loaded area, shown as the right-hand edge of Figure 6. Displacements are shown by the curvature of the upper surface of the grid. Resultant strain energy distribution is shown by the grayscale infill. In general, light colors represent high values of strain energy, which correspond to high stresses. Darker regions represent low stress areas.

The FEM code was run, for this example, assuming that there was no slip at the bed boundary or shear within the sand. Various systems were compared with different relative thicknesses of hard and soft rock. If most of the system is composed of soft rock, as in Figure 6, a displacement is induced in the hard layer which is much larger than that which would result from the same load applied to a uniform high-modulus material. The large strain causes an accompanying very high stress as determined by the modulus of the hard material. Analyzing the strain energy in terms of the von Mises or Mohr-Coulomb failure criterion shows that the soft sediment must fail in shear at the bed boundary. As discussed previously, once shear failure occurs, the two beds (hard and soft) deform as separate, decoupled units. Displacements in each unit are caused only by the pressure acting on that unit. Also, after shear failure occurs, displacements in the soft sand cannot be transmitted across the hard streak, thus have no effect on stresses or fracture widths in the soft sand on the opposite side of the hard streak. Displacements in the soft rock are also not transmitted to the hard streaks. This results in very narrow widths in the hard rock sections and potentially large width variations in layered systems.

This discussion suggests several things about fracture height, width, and treating pressure in layered systems with large modulus contrasts. First, shear slippage or failure may be fairly common in soft, weak rocks. This leads to better height containment, even by very thin beds, if slippage occurs at bed boundaries. Lack of elastic coupling throughout the system results in much narrower created fracture widths, in both hard and soft regions, than previously expected. Loss of energy at the shear planes minimizes stress concentrations in the fracture process zone, requiring much higher fluid pressures to induce fracture growth. These results are consistent with virtually all observations concerning fracturing in soft sediments.

## Example of Model Results – M-site 4c

As an example of the results obtained from an elastically decoupled simulator, data from the GRI/DOE M-site was utilized. To illustrate the improved containment predicted by the decoupled model, and the influence of viscous pressure gradients in narrow fractures, the M-site 4c treatment was modeled. All data used in the study were obtained directly from published GRI/DOE information, including rock elastic properties, stress profile, and rate schedule.[15, 16] The model includes the effects of varying fluid rheology and pressure dependent leakoff to simulate opening of secondary fissures. Figure 7 shows the surface and bottomhole pressure data recorded during the test compared to the model results. Some of the pressure response, particularly the high treating pressures noted after shut-in during crosslinked gel injection,

is due to static fluid gelation and the development of an apparent yield-point during shut-in and cannot be modeled with existing software. However, in general the model provides a good qualitative match of the observed pressure behavior through the two water injections and both shut-ins, followed by two periods of gel injection with their associated shut-ins.

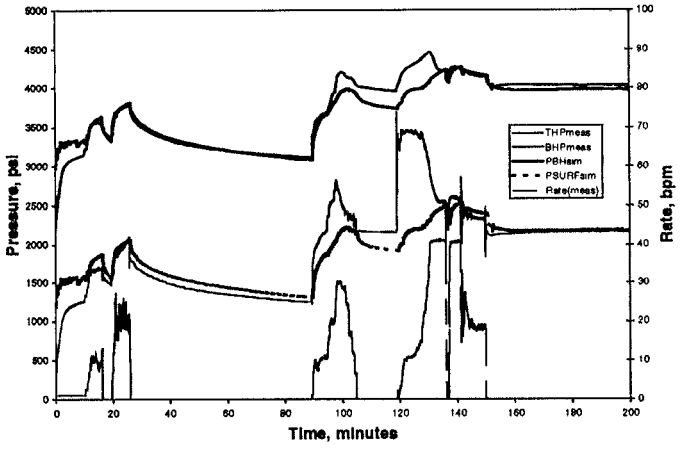


**Figure 7: Pressure match for the M-site 4c injection**

The more interesting result of the modeling study is the predicted fracture geometry and height containment for the first pair of injections (water) and the second (crosslinked gel) injection set. Previous attempts at modeling these data have suggested that the observed height containment is better than predicted using elastically coupled fracture models. The rapid development of fracture length has also been difficult to account for.

Using the elastically decoupled shear-slippage model the observed fracture geometry is easily matched. Figure 8 shows the predicted fracture width profile at the end of the water injection. At early times the fracture is actually contained in the upper half of the C sand and grows to about 500 feet of half-length during the first 16 minutes of injection (prior to the first shut-in) as indicated by the microseisms recorded during the 3c injection stage at M-site.[15] Very few microseisms were observed during the early 4c injection stage. The second water injection stage extended the fracture height into the lower half of the C sand, but did not create substantial additional length.

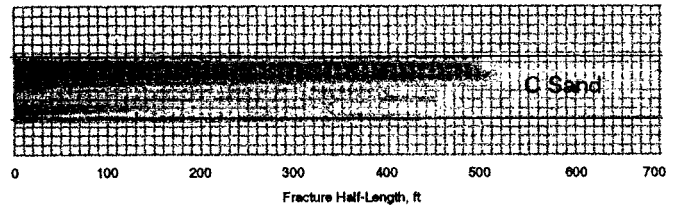


**Figure 8: Modeled width profile after water injection**

Figure 9 shows the predicted fracture width profile at the peak injection rate during the crosslinked fluid phase. During this part of the injection no additional length was created but fracture height grew into the overlying beds and secondary (fissure) leakoff increased. The predicted containment profile agrees very well with the observed pattern of microseismic activity during each injection stage.

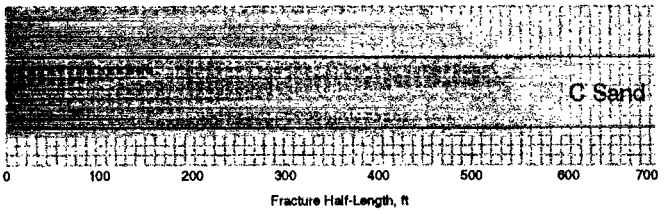


**Figure 9: Modeled width profile after crosslinked gel injection**

The model-predicted fracture widths also agree qualitatively with the observed inclinometer readings made during the 4c injection cycle. The maximum created fracture width during the water injection phase was only 0.10 inches while fracture widths up to 0.26 inches were predicted during gel injection. Inclinometer data suggest a substantial increase in fracture width during the later gel injection stage, compared to the widths observed during water injection. The strong dependence of width on fluid rheology results from the decoupling of the fracture deformation from the fracture tip process-zone. Under this assumption the fracture behaves as a viscous-dominated system. Fracture extension at the tip occurs only when local fracture fluid pressures exceed closure stress (and tensile strength) at any point along the fracture perimeter.

## Conclusions and Implications

Field observations have been made that suggest that fracture height containment is better than predicted by linear elastic fracture mechanics (LEFM) models. It has been suggested that containment mechanisms may exist which have not been previously identified. Treating pressures have been observed in many cases, especially in soft sediments and naturally fractured reservoirs, which appear anomalously high. This paper has introduced several physically simple mechanisms that can contribute to improved containment and higher treating pressures. The mechanisms can be supported by all available field observations and are consistent with rock failure analysis measurements. The present level of work is sufficient to indicate that the effects of shear failure during hydraulic fracturing should be further investigated. Where possible, these effects should be included in existing design simulators. Some major conclusions, which can be drawn from the preliminary observations presented here, are:

1. Microseismic monitoring suggests that shear failure occurs during hydraulic fracturing, in at least some cases.
2. When shear slippage occurs, plane-strain and linearly-elastic surface integral solutions over-estimate created frac width and process-zone stress.
3. The surface integral solution can be modified to account for shear dampening of the displacement field.
4. Shear-dampened width solutions can lead to narrower

created widths, better height containment, and higher treating pressures.

5. Shear failure and slip can occur at bed boundaries, especially in soft sediments.

6. Slip at bed boundaries can lead to narrower widths, improved containment, high treating pressure, and large width variations.

7. Shear slip can be included in fracture design models and its effects evaluated. Unfortunately, the occurrence and exact location of slip planes cannot be well predicted.

## Acknowledgements

The authors would like to thank Dr. Mike Conway of Stim Lab, Inc. for his valuable discussions on this, and other topics. We would also like to thank W. R. Dahl for his support with ALGOR, and the management of Marathon Oil Company for the time to pursue and publish this work.

## References

1. Griffith, A. A.: "The Theory of Rupture," Int. Congress of Applied. Mech., Proc., Delft, pp 55-63 (1924).
2. Sneddon, I. N.: "The Distribution of Stress in the Neighborhood of a Crack in an Elastic Solid," *Proc.* Royal Soc., A187, pp 229-267 (1946).
3. Sneddon, I. N.: "The Opening of a Griffith Crack Under Internal Pressure," *Quart. Appl. Math.*, v4, pp 262-267 (1946).
4. England, A. H. and Green, A. E.: "Some Two Dimensional Punch and Crack Problems in Classical Elasticity," *Proc.* Cambridge Phil. Soc., v59, pp 489-500 (1963).
5. Timoshenko, S. P. and Goodier, J. N.: *Theory of Elasticity, Third Ed.*, Eng. Soc. Mon., McGraw-Hill, New York City (1970) 404.
6. Geertsma, J. and De Klerk, F.: "A Rapid Method of Predicting Width and Extent of Hydraulically Induced Fractures," *JPT* (Dec. 1969) 1571.
7. Nordgren, R. P.: "Propagation of a Vertical Hydraulic Fracture," *SPEJ* (Aug. 1972) 306.
8. Geertsma, J. and Haafkens, R.: "A Comparison of the Theories for Predicting Width and Extent of Hydraulically Induced Fractures," *Trans. ASME, J. of Energy Resources Tech.*, (March 1979) 8.
9. Barree, R. D.: "A Practical Numerical Simulator for Three-Dimensional Fracture Propagation in Heterogeneous Media," paper SPE 12273 presented at the 1983 SPE Symposium on Reservoir Simulation, San Francisco, CA, Nov. 15-18.
10. Warpinski, N.R., Moschovidis, Z.A., Parker, C.D, Abou-Sayed, I.S.: "Comparison Study of Hydraulic Fracturing Models: Test Case-GRI- Staged Field Experiment No. 3," paper SPE 25890 presented at the Rocky Mountain Regional/Low Permeability Reservoirs Symposium, Denver, CO, U.S.A., April 12-14
11. Clifton, R. J., Abou-Sayed, A.S.: "On the Computation of the Three-Dimensional Geometry of Hydraulic Fractures," paper SPE 7943 presented at the SPE of AIME Symposium on Low Permeability Gas Reservoirs, May 20-22, 1979.
12. Warpinski, N. R.: "Interpretation of Hydraulic Fracture Mapping Experiments," paper SPE 27985 presented at the Tulsa Centennial Petroleum Engineering Symposium, Tulsa, OK, Aug. 1994.
13. Wright, C. A., Davis, E. J., Minner, W. A., Ward, J. F., Weijer, L., Schell, E. J., and Hunter, S. P.: "Surface Tiltmeter Fracture Mapping Reaches New Depths – 10,000 feet, and Beyond?" paper SPE 39919 presented at the Rocky Mountain Regional/Low Permeability Reservoirs Symposium, Denver, CO, Apr. 5-8, 1998.
14. Warpinski, N.R., Teufel, L.W.: "Influence of Geologic Discontinuities on Hydraulic Fracture Propagation," *JPT* (Feb 1987) 209.
15. Warpinski, N. R., Branagan, P. T., Peterson, R. E., Fix, J. E., Uhl, J. E., Engler, B. P., and Wilmer, R.: "Microseismic and Deformation Imaging of Hydraulic Fracture Growth and Geometry," paper SPE 38573 presented at the Annual Technical Conference and Exhibition, San Antonio, TX, Oct. 5-8, 1997.
16. *Forum: M-Site Experiments – Data Interpretation and Implications*, CD produced by Gas Research Institute, Houston, TX, Nov. 5-6, 1997.

## Nomenclature

$S_d$ = shear dampening radius, L, ft